Available online at www.eccomasproceedia.org
Eccomas Proceedia SMART (2023) 526-537

ECCOMAS
Proceedia

X ECCOMAS Thematic Conference on Smart Structures and Materials
SMART 2023
D.A. Saravanos, A. Benjeddou, N. Chrysochoidis and T. Theodosiou (Eds)

# SEMI-ACTIVE MODAL CONTROL BASED ON THE ENERGY TRANSFER BETWEEN STRUCTURAL VIBRATION MODES

**MARIUSZ OSTROWSKI*, BARTLOMIEJ BLACHOWSKI, GRZEGORZ MIKUŁOWSKI, AND ŁUKASZ JANKOWSKI**

Institute of Fundamental Technological Research, Polish Academy of Sciences (IPPT PAN)
Warsaw, Poland
e-mail: mostr@ippt.pan.pl

**Abstract.** Vibration control is a crucial issue in engineering, necessitating the continuous development and refinement of effective control strategies. In the present study, a semi-active control methodology utilizing lockable joints is investigated. The lockable joints provide a modal coupling effect, resulting in controlled energy transfer between vibration modes. Numerical simulations demonstrate that energy can be transferred to higher-order vibration modes and rapidly dissipated through inherent material damping or transferred to a preselected vibration mode for energy harvesting.

**Key words:** Semi-active modal control, Smart Structures, Lockable joints, Energy transfer, Vibration damping

## 1 INTRODUCTION

Due to its significance in the maintenance and safety of engineering and civil structures, vibration control has been developed and refined for decades. Among various methodologies, semi-active control offers performance close to fully active control while retaining the advantages of passive vibration mitigation methods, such as the absence of destabilization risks and no requirement for an efficient power source [1].

Typically, semi-active control strategies are designed to dissipate vibration energy in controlled devices [2]. Despite the effectiveness of this approach, it has certain limitations, such as operational wear on the device, load capacity constraints, and maximum rates of energy dissipation. Consequently, efforts have been directed towards designing devices capable of transmitting significant loads. For example, Laflamme et al. proposed a concept of a semi-active friction device for mitigation of vibrations in buildings [3].

In contrast to many local energy dissipation approaches, a recently proposed methodology called prestress–accumulation release (PAR) enables energy dissipation in the entire structural volume [4, 5]. This control strategy employs lockable joints, which, during the motion of the structure, remain in a locked state, causing deformation and accumulation of strain energy in


Peer-review under responsibility of the organizing committee of SMART 2023.
doi: 10.7712/150123.9807.444377

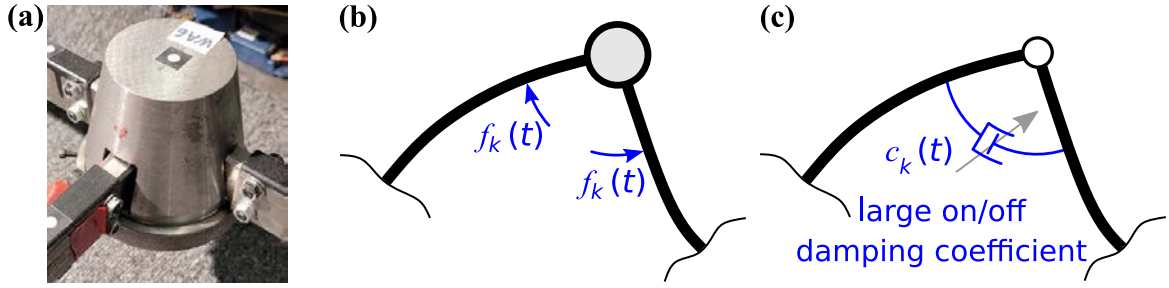


**Figure 1:** Dynamics of $k$th lockable joint: (a) real prototype of the lockable joint, (b) pair of self-equilibrated moments present during locking of the joint and (b) viscous model of the locking effect

higher-order modes. When this energy reaches its maximum value, the joints are suddenly unlocked, and the strain energy is released into higher-order vibration modes, where it is rapidly dissipated through material damping. Despite the satisfactory performance of this approach, it relies solely on local strain measurements, which results in unlocking the joints at local strain energy maxima. Ostrowski et al. proposed a modal approach for the dissipation of vibration energy, which also employs lockable joints and transfers energy from lower-order, weakly damped, vibration modes to higher-order modes but is less dependent on the local strain [6].

This paper investigates a modal energy transfer-based approach that employs lockable joints. Two potential applications are considered: vibration damping and energy harvesting. In the former case, energy is transferred to higher-order vibration modes, whereas in the latter, energy is transferred to a preselected mode that can effectively cooperate with an energy harvester.

## 2 SEMI-ACTIVE CONTROL METHODOLOGY

### 2.1 System dynamics

#### 2.1.1 Lockable joints with an on/off ability to transmit the bending moment

A flexible multi-degree-of-freedom (MDOF) structure is considered. It is equipped with and controlled through lockable joints. An example of such a lockable joint is shown in Figure 1a. The un/locking effect is achieved through the sudden activation of a piezo-stack, which controls the clamping force between friction components. The friction force is sufficiently large to prevent relative rotational motion between structural members connected via the lockable joint.

The dynamics of the structure, with either fully locked (as in a rigid connection) or fully unlocked (as in a hinge) joints, is assumed to satisfy the following constraints:

$$u_k(t)(\dot{q}_i(t) - \dot{q}_j(t)) = 0, \quad u_k(t) \in \{0, 1\} \tag{1}$$

where $u_k$ is the control signal of the $k$th lockable joint (if equal to one, then the joint is locked; if zero, then unlocked), $i$ and $j$ denote the rotational degrees of freedom (DOFs) of the beams involved in the $k$th lockable joint, and $q_i(t)$ represents the rotational displacement. Constraint (1) is applied to the rotational velocities rather than the displacements, as the joint can be locked at

any relative angle between the connected beams. The locking effect can be described by a pair of self-equilibrated moments applied to the rotational DOFs involved in the lockable joints, as illustrated in Figure 1b.

The transient state between fully unlocked and fully locked states is very short; hence, energy dissipation in the lockable joint is negligible. Therefore, in this study, nonlinear friction effects are disregarded. A model based on a viscous damper, as depicted in Figure 1c, is employed to simplify the structural model. This viscous damper ensures that condition (1) is closely satisfied, which is possible due to the potentially large values of $c_k(t) = c_{\max} u_k(t)$, where $c_{\max}$ is a constant large damping parameter. In this case, the bending moment transmitted via the lockable joint is described by Equation (2)

$$f_k(t) = -c_{\max} u_k(t)(\dot{q}_i(t) - \dot{q}_j(t)). \tag{2}$$

### 2.1.2 Motion of MDOF structure equipped with lockable joints

The structural motion is described by equation of motion below:

$$\mathbf{M}\ddot{\mathbf{q}}(t) + \mathbf{C}\dot{\mathbf{q}}(t) + \mathbf{K}\mathbf{q}(t) = \mathbf{L}\mathbf{f}(t) + \mathbf{d}(t) \tag{3}$$

In Equation (3), $\mathbf{M}$, $\mathbf{C}$ and $\mathbf{K}$ are mass, material damping, and stiffness matrices, respectively, $\mathbf{q}(t)$ is the displacement vector (including both translation and rotation), and $\mathbf{f}(t) = \begin{bmatrix} f_1(t) & f_2(t) & \cdots & f_{N_k}(t) \end{bmatrix}^{\mathrm{T}}$ is the vector of bending moments transmitted via lockable joints,

$$\begin{aligned} \mathbf{L} &= \begin{bmatrix} \mathbf{l}_1(t) & \mathbf{l}_2(t) & \cdots & \mathbf{l}_{N_k}(t) \end{bmatrix}, \\ \mathbf{l}_k &= \begin{bmatrix} 0 & \cdots & 0 & 1 & 0 & \cdots & 0 & -1 & 0 & \cdots & 0 \end{bmatrix}^{\mathrm{T}} \end{aligned} \tag{4}$$

is a transformation matrix that selects the DOFs involved in the lockable joints and ensures self-equilibrium of the pair of moments in each $k$th joint, as shown in Figure 1b, and $\mathbf{d}(t)$ is the vector of external loads. A proportional material dampling model is employed.

To describe the energy transfer between vibration modes and develop an appropriate control law, the structural motion is expressed in terms of modal coordinates $\boldsymbol{\eta}(t)$ as follows:

$$\mathbf{q}(t) = \boldsymbol{\Phi}\boldsymbol{\eta}(t), \tag{5}$$

where $\boldsymbol{\Phi} = \begin{bmatrix} \boldsymbol{\phi}^{(1)} & \boldsymbol{\phi}^{(2)} & \cdots & \boldsymbol{\phi}^{(N_m)} \end{bmatrix}$ is the modal matrix collecting the mode shapes $\boldsymbol{\phi}^{(m)}$ normalized with respect to the mass matrix. After substitution Equation (5) into (3) and left-multiplying by the transposed modal matrix, the modal equation of motion is obtained:

$$\ddot{\boldsymbol{\eta}}(t) + 2\mathbf{Z}\boldsymbol{\Omega}\dot{\boldsymbol{\eta}}(t) + \boldsymbol{\Omega}^2\boldsymbol{\eta}(t) = \boldsymbol{\Phi}^{\mathrm{T}}\mathbf{L}\mathbf{f}(t) + \boldsymbol{\Phi}^{\mathrm{T}}\mathbf{d}(t), \tag{6}$$

where $\mathbf{Z} = \operatorname{diag}\left(\begin{bmatrix} \zeta^{(1)} & \zeta^{(2)} & \cdots & \zeta^{(N_m)} \end{bmatrix}\right)$ and $\boldsymbol{\Omega} = \operatorname{diag}\left(\begin{bmatrix} \omega^{(1)} & \omega^{(2)} & \cdots & \omega^{(N_m)} \end{bmatrix}\right)$ are diagonal matrices containing modal damping factors and natural frequencies, respectively.

After substituting Equation (2) into each elements of the vector $\mathbf{f}(t)$, the modal equation of motion for a specific vibration mode can be written as follows:

$$\begin{aligned}\ddot{\eta}_m(t) + 2\zeta^{(m)}\omega^{(m)}\dot{\eta}_m(t) + \omega^{(m)2}\eta_m(t) &= \boldsymbol{\phi}^{(m)\mathrm{T}} \sum_{k=1}^{N_k} \mathbf{l}_k f_k(t) + \boldsymbol{\phi}^{(m)\mathrm{T}}\mathbf{d}(t) \\ &= -c_{\max}\boldsymbol{\phi}^{(m)\mathrm{T}} \sum_{k=1}^{N_k} u_k(t)\mathbf{l}_k\mathbf{l}_k^{\mathrm{T}}\boldsymbol{\Phi}\dot{\boldsymbol{\eta}}(t) + \boldsymbol{\phi}^{(m)\mathrm{T}}\mathbf{d}(t)\end{aligned} \tag{7}$$

The row vector $\boldsymbol{\phi}^{(m)\mathrm{T}}\mathbf{l}_k\mathbf{l}_k^{\mathrm{T}}\boldsymbol{\Phi}$ is typically full. Thus, locking any joint results in a modal coupling effect, leading to a component of the modal force acting on the $m$th modal coordinate.

### 2.1.3 Modal energy transfer

The mechanical energy $E(t)$ of the structure is the sum of mechanical energies associated with particular vibration modes $E_m(t)$, as shown in the following equation:

$$\begin{aligned}E(t) &= \frac{1}{2}\dot{\mathbf{q}}^{\mathrm{T}}(t)\mathbf{M}\dot{\mathbf{q}}(t) + \frac{1}{2}\mathbf{q}^{\mathrm{T}}(t)\mathbf{K}\mathbf{q}(t) = \frac{1}{2}\dot{\boldsymbol{\eta}}^{\mathrm{T}}(t)\underbrace{\boldsymbol{\Phi}^{\mathrm{T}}\mathbf{M}\boldsymbol{\Phi}}_{\mathbf{I}}\dot{\boldsymbol{\eta}}(t) + \frac{1}{2}\boldsymbol{\eta}^{\mathrm{T}}(t)\underbrace{\boldsymbol{\Phi}^{\mathrm{T}}\mathbf{K}\boldsymbol{\Phi}}_{\boldsymbol{\Omega}^2}\boldsymbol{\eta}(t) = \\ &= \sum_{m=1}^{N_m}\frac{1}{2}\left(\dot{\eta}_m^2(t) + \omega^{(m)2}\eta_m^2(t)\right) = \sum_{m=1}^{N_m} E_m(t).\end{aligned} \tag{8}$$

It is evident that, in the case of free vibration, the energy of any vibration mode can increase at the expense of other modal energies, as caused by the modal coupling effect. The increment of the $m$th modal energy is

$$\dot{E}_m(t) = \dot{\eta}_m(t)\left(\ddot{\eta}_m(t) + \omega^{(m)2}\eta_m(t)\right). \tag{9}$$

After substituting Equation (7) into Equation (9), the increment of the $m$th modal energy can be explicitly expressed as the sum of three components:

$$\begin{aligned}\dot{E}_m(t) &= \dot{\eta}_m(t)\left(-c_{\max}\sum_{k=1}^{N_k} u_k(t)\boldsymbol{\phi}^{(m)\mathrm{T}}\mathbf{l}_k\mathbf{l}_k^{\mathrm{T}}\boldsymbol{\Phi}\dot{\boldsymbol{\eta}}(t) - 2\zeta^{(m)}\omega^{(m)}\dot{\eta}_m(t) + \boldsymbol{\phi}^{(m)\mathrm{T}}\mathbf{d}(t)\right) \\ &= \underbrace{-c_{\max}\dot{\eta}_m(t)\sum_{k=1}^{N_k} u_k(t)\boldsymbol{\phi}^{(m)\mathrm{T}}\mathbf{l}_k\mathbf{l}_k^{\mathrm{T}}\boldsymbol{\Phi}\dot{\boldsymbol{\eta}}(t)}_{\dot{W}_m(t)} \underbrace{-\,2\zeta^{(m)}\omega^{(m)}\dot{\eta}_m^2(t)}_{-\dot{E}_m^{\mathrm{loss}}(t)} + \underbrace{\dot{\eta}_m(t)\boldsymbol{\phi}^{(m)\mathrm{T}}\mathbf{d}(t)}_{\dot{W}_m^{\mathrm{ext}}(t)}.\end{aligned} \tag{10}$$

In the equation above, $W_m(t)$ represents the energy transferred to the $m$th vibration mode from all remaining modes, $E_m^{\mathrm{loss}}(t)$ is the energy dissipated in material damping, and $W_m^{\mathrm{ext}}(t)$ is the work of external loads done on the $m$th modal coordinate. The derivative of $W_m(t)$ is called the modal energy transfer rate to the $m$th vibration mode. If $\dot{W}_m^{\mathrm{ext}}(t)$ takes a negative sign, then the energy flow has a direction from the $m$th vibration mode to the remaining ones.

## 3 SEMI-ACTIVE CONTROL OF THE MODAL ENERGY TRANSFER

In this section, the proposed control methodology is described for two applications: (1) semi-active vibration damping, and (2) energy harvesting. In the former case, mechanical energy is transferred from monitored, low-order vibration modes, characterized by low material damping, to high-order modes that typically exhibit significant damping. This triggers rapid energy dissipation in the entire volume of the structure. In the latter case, vibration energy is transferred to a selected mode that effectively cooperates with the energy harvester attached to the structure.

### 3.1 Instantaneously optimal control law

Developing control that is optimal in the sense of Pontryagin's principle is challenging for systems equipped with devices such as lockable joints [5]. Therefore, an instantaneously optimal approach is employed. For the vibration attenuation application, a Lyapunov function is defined as the weighted sum of modal energies of $N_p$ monitored vibration modes:

$$V(t) = \sum_{p=1}^{N_p} \alpha_p E_p(t) \tag{11}$$

Weights $\alpha_p$ decrease with the increasing order of the vibration mode, e.g., $\alpha_p = \omega_p^{-2}$. This is due to the fact that low-order vibration modes, characterized by low material damping, should be attenuated with higher priority. The control providing the steepest descent of the Lyapunov function at each time instance is sought. $\dot{V}(t)$ is a weighted sum of modal energy derivatives, see Equation (10). At any time instance $t$, the control directly affects only the term representing the modal energy transfer rate. Thus, the optimization problem can be formulated as:

$$\begin{aligned} &\text{for current } t \text{ find} && \mathbf{u}(t) \in \{0,1\}^{N_k} \\ &\text{to minimize} && \dot{V}_W(t), \end{aligned} \tag{12}$$

where

$$\dot{V}_W(t) = \sum_{p=1}^{N_p} \alpha_p \dot{W}_p(t). \tag{13}$$

From Equations (7) and (10), it follows that the weighted modal energy transfer rate represented by $\dot{V}_W(t)$ is the sum of weighted modal energy transfer rates through each lockable joint:

$$\begin{aligned} \dot{V}_W(t) &= -\sum_{p=1}^{N_p} \alpha_p c_{\max} \dot{\eta}_p(t) \sum_{k=1}^{N_k} u_k(t) \boldsymbol{\phi}^{(p)\mathrm{T}} \mathbf{l}_k \mathbf{l}_k^{\mathrm{T}} \boldsymbol{\Phi} \dot{\boldsymbol{\eta}}(t) = \\ &= \sum_{p=1}^{N_p} \alpha_p \sum_{k=1}^{N_k} \dot{W}_{pk}(t) = \sum_{k=1}^{N_k} \sum_{p=1}^{N_p} \alpha_p \dot{W}_{pk}(t) = \sum_{k=1}^{N_k} \dot{V}_{Wk}(t), \end{aligned} \tag{14}$$

where

$$\dot{W}_{pk}(t) = -c_{\max} u_k(t) \dot{\eta}_p(t) \boldsymbol{\phi}^{(p)\mathrm{T}} \mathbf{l}_k \mathbf{l}_k^{\mathrm{T}} \boldsymbol{\Phi} \dot{\boldsymbol{\eta}}(t) \tag{15}$$

is the modal energy transfer rate to the $p$th mode through the $k$th lockable joint, and

$$\dot{V}_{Wk}(t) = \sum_{p=1}^{N_p} \alpha_p \dot{W}_{pk}(t) = -c_{\max} u_k(t) \sum_{p=1}^{N_p} \alpha_p \dot{\eta}_p(t) \boldsymbol{\phi}^{(p)\mathrm{T}} \mathbf{l}_k \mathbf{l}_k^{\mathrm{T}} \boldsymbol{\Phi} \dot{\boldsymbol{\eta}}(t) \tag{16}$$

is the sum of weighted modal energy transfer rates to the monitored modes through the $k$th lockable joint.

The calculations above lead to the conclusion that the optimization problem in Equation (12) can be solved by independently controlling each joint with the following control law:

$$u_k = \begin{cases} 1 & \text{for } \dot{V}_{Wk}(t) < 0 \\ 0 & \text{otherwise} \end{cases}, \quad u_k = 1, 2, \ldots N_k. \tag{17}$$

In order to transfer energy to the preselected vibration mode, as is the case for the energy harvesting application, the corresponding weight $\alpha_r$ should be negative and have a significant absolute value in relation to the remaining weights. Such a selection of the weight $\alpha_r$ ensures that the energy is effectively transferred to the preselected vibration mode without transferring a significant amount to the higher-order modes. Energy transferred to the higher-order modes is considered wasted in the case of the energy harvesting application. It is worth noting that pursuing negative weights in Equation (11) does not cause destabilization of the system in free vibration due to the fact that the control is of the semi-active type. Lockable joints do not introduce any energy to the structure.

### 3.2 Measured quantities and control algorithm

In order to implement the control law described by Equation (17), the weighted modal energy transfer rate through each $k$th lockable joint, $\dot{V}_{Wk}(t)$, must be estimated from measurement. Inspection of Equation (16) shows that $\dot{V}_{Wk}(t)$ depends on all modal velocities. This results from the fact that bending moments $f_k(t)$, which cause the interaction between vibration modes as shown in Equation (7), depend on the local curvature of the beams connected to the joints when locked. These local curvatures contain not only lower-order but also higher-order mode shape components. On the other hand, only the first $N_p$ vibration modes are monitored due to the available number of sensors and other equipment limitations.

Taking into account the problem described above, the weighted modal energy transfer rate, $\dot{\widehat{V}}_{Wk}(t)$, is calculated using different equations depending on the current state of the joint (locked or unlocked). Form the relation between the modal coupling term and bending moments shown in Equation (7), it follows that $\dot{\widehat{V}}_{Wk}(t)$ can be calculated using the first $N_p$ estimated modal velocities and the estimated bending moment, $\widehat{f}_k(t)$, when the $k$th joint is in the locked state. Then, equation below is used:

$$\dot{\widehat{V}}_{Wk}(t) = \sum_{p=1}^{N_p} \alpha_p \dot{\widehat{\eta}}_p(t) \boldsymbol{\phi}^{(p)\mathrm{T}} \mathbf{l}_k \widehat{f}_k(t) = \dot{\widehat{\boldsymbol{\eta}}}_{\mathrm{M}}^{\mathrm{T}}(t) \mathbf{W}_\alpha \boldsymbol{\Phi}_{\mathrm{M}}^{\mathrm{T}} \mathbf{l}_k \widehat{f}_k(t), \tag{18}$$

where $\dot{\widehat{\boldsymbol{\eta}}}_{\mathrm{M}}(t) = \left[\dot{\widehat{\eta}}_{\mathrm{M}1}(t) \quad \dot{\widehat{\eta}}_{\mathrm{M}2}(t) \quad \cdots \quad \dot{\widehat{\eta}}_{\mathrm{M}N_p}(t)\right]^{\mathrm{T}}$ is the vector of estimated modal velocities, $\mathbf{W}_\alpha = \mathrm{diag}\left(\begin{bmatrix}\alpha_1 & \alpha_2 & \cdots & \alpha_{N_p}\end{bmatrix}^{\mathrm{T}}\right)$ is the diagonal weighting matrix, and $\boldsymbol{\Phi}_{\mathrm{M}}$ is the modal matrix truncated to the $N_p$ monitored modes. Following the control law (17), the currently locked $k$th joint should be unlocked when $\dot{\widehat{V}}_{Wk}(t)$, calculated as above, becomes positive (i.e., energy flow becomes unprofitable).

For the joint being currently in the unlocked state, $f_k(t) = 0$, hence using Equation (18) is then invalid. However, it is possible to calculate $\dot{\widehat{V}}_{Wk}(t)$ that will appear if the $k$th joint is suddenly locked. This can be done by substituting $u(t) = 1$ in Equation (16) and truncating the modal parameters to the $N_p$ monitored modes:

$$\begin{aligned}\dot{\widehat{V}}_{Wk}(t) &= -c_{\max}\sum_{p=1}^{N_p}\alpha_p\dot{\widehat{\eta}}_p(t)\boldsymbol{\phi}^{(p)\mathrm{T}}\mathbf{l}_k\mathbf{l}_k^{\mathrm{T}}\boldsymbol{\Phi}_{\mathrm{M}}\dot{\widehat{\boldsymbol{\eta}}}_{\mathrm{M}}(t) = \\ &= -c_{\max}\dot{\widehat{\boldsymbol{\eta}}}_{\mathrm{M}}^{\mathrm{T}}(t)\mathbf{W}_\alpha\boldsymbol{\Phi}_{\mathrm{M}}^{\mathrm{T}}\mathbf{l}_k\mathbf{l}_k^{\mathrm{T}}\boldsymbol{\Phi}_{\mathrm{M}}\dot{\widehat{\boldsymbol{\eta}}}_{\mathrm{M}}(t).\end{aligned} \tag{19}$$

Here, truncating the modal parameters to the first $N_p$ monitored modes does not introduce significant errors to $\dot{\widehat{V}}_{Wk}(t)$, as opposed to the situation when any joint is in the locked state. When a joint is locked, the higher-order vibration modes are pre-stressed and do not vibrate with their natural frequencies (quasi-static motion), and consequently, these modes are not yet significantly mitigated by material damping. Upon unlocking the joint, these vibration modes begin to vibrate freely and are quickly mitigated by material damping, rendering their participation in structural motion negligible before the next joint lock occurs. Condition (18) and (19) are used alternately, depending on the current state of the joint.

In the equations above, $\widehat{f_k}(t)$ can be obtained from the measurement of strains on the beam in the vicinity of the $k$th lockable joint:

$$\widehat{f_k}(t) = -\frac{2EI}{h}\varepsilon_{\mathrm{M}k}(t), \tag{20}$$

where $E$, $I$, and $h$ are the Young's modulus, moment of inertia, and height of the cross-section, respectively. Additionally, $\varepsilon_{\mathrm{M}k}(t) = \left[\varepsilon_{\mathrm{M}k}^{\mathrm{I}}(t) - \varepsilon_{\mathrm{M}k}^{\mathrm{II}}(t)\right]/2$ represents the difference of strains measured, for example, using strain gauges at the bottom and top surfaces of the beam, which allows for the rejection of the longitudinal strain component.

The modal velocities of the monitored vibration modes, $\dot{\widehat{\boldsymbol{\eta}}}_{\mathrm{M}}(t)$, are estimated using the modal filtering technique, as demonstrated by Equation (21).

$$\dot{\widehat{\boldsymbol{\eta}}}_{\mathrm{M}}(t) = (\mathbf{L}_{\mathrm{s}}\boldsymbol{\Phi}_{\mathrm{M}})^{+}\dot{\mathbf{q}}_{\mathrm{M}}(t), \tag{21}$$

where $(\cdot)^{+}$ denotes the Moore–Penrose pseudoinverse of the matrix, $\mathbf{L}_{\mathrm{s}}$ is a Boolean matrix selecting sensor locations, and $\dot{\mathbf{q}}_{\mathrm{M}}(t)$ represents the measured velocities at these locations. If the number of sensors is greater than the number of monitored vibration modes, then Equation (21)

provides the least-square estimate. If the number of sensors is equal to the number of monitored vibration modes, a reciprocal matrix is used instead of the pseudoinverse. Sensor locations, encoded by matrix $\mathbf{L}_\mathrm{s}$, can be selected according to the methodology described in [7], which maximizes the determinant of the corresponding Fisher information matrix.

The control algorithm that implements the proposed instantaneously optimal control methodology is presented in the form of pseudocode in Algorithm 1. To prevent the influence of noise on control, thresholds $\kappa_1$ and $\kappa_2$ are added to the conditions used to lock/unlock the joint (lines 4 and 7 of the algorithm). After each lock/unlock of any joint, the algorithm is paused for a preselected short time until higher order vibration modes are mitigated to avoid the measurement spillover effect (lines from 11 to 15 of the algorithm).

## 4 NUMERICAL EXAMPLES

This section demonstrates the performance of the proposed control method. The same excitation and structure are used in both vibration damping and directed energy transfer examples.

The scheme of the structure under consideration is shown in Figure 2a. The structure is equipped with two lockable joints at the ends of the top horizontal beam. Each bay of the structure has dimensions of 0.6×0.6 m, and the beam cross-section is 10×8 mm (8 mm in plane of the structure). The Young's modulus $E = 210$ GPa (steel), the material density $\rho = 7860$ kg/m$^3$ (steel), and the mass of the lockable joint is 1.2 kg. A finite element (FE) model with one FE per each bay (9 FEs in total) is used for simulation. Each FE is a beam element based on Euler–Bernoulli beam theory, with four DOFs (in plane vibration without lengthening) and cubic shape functions. The FE model has 11 DOFs in total. The first three vibration

**Algorithm 1** Algorithm for realisation of the energy transfer between vibration modes

1: Estimate $\dot{\widehat{\boldsymbol{\eta}}}_\mathrm{M}(t)$ and $\widehat{f}_k(t),\ k = 1, 2, \ldots N_k$
2: **for** $k = 1, 2, \ldots N_k$ **do** ▷ For each lockable joint
3: $u_k^{\mathrm{prev}} \leftarrow u_k$
4: **if** $u_k(t) == 0$ **and** $-c_{\max} u_k(t) \dot{\widehat{\boldsymbol{\eta}}}_\mathrm{M}^\mathrm{T}(t) \mathbf{W}_\alpha \boldsymbol{\Phi}_\mathrm{M}^\mathrm{T} \mathbf{l}_k \mathbf{l}_k^\mathrm{T} \boldsymbol{\Phi}_\mathrm{M} \dot{\widehat{\boldsymbol{\eta}}}_\mathrm{M}(t) < -\kappa_1$ **then**
5: $u_k(t) \leftarrow 1$ ▷ Lock $k$th joint
6: **end if**
7: **if** $u_k(t) == 1$ **and** $\dot{\widehat{\boldsymbol{\eta}}}_\mathrm{M}^\mathrm{T}(t) \mathbf{W}_\alpha \boldsymbol{\Phi}_\mathrm{M}^\mathrm{T} \mathbf{l}_k \widehat{f}_k(t) \geq \kappa_2$ **then**
8: $u_k(t) \leftarrow 0$ ▷ Unlock $k$th joint
9: **end if**
10: **end for**
11: **if** any($u_k^{\mathrm{prev}} == 1$ and $u_k == 0$) **then** ▷ Any joint unlocked?
12: Wait $t_{\mathrm{unlock}}$ ▷ Wait until higher-order modes are mitigated
13: **else if** any($u_k^{\mathrm{prev}} == 0$ and $u_k == 1$) **then** ▷ Any joint locked?
14: Wait $t_{\mathrm{lock}}$ ▷ Wait until higher-order modes are mitigated
15: **end if**
16: Return to line no. 1

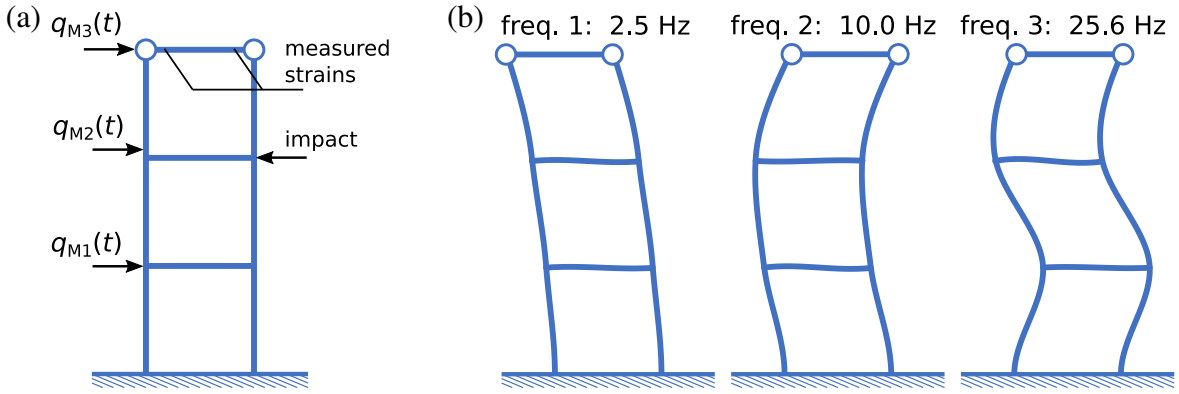


**Figure 2:** Investigated structure: (a) scheme with indicated locations of sensors and impact, and (b) monitored vibration modes accompanied with corresponding undamped natural frequencies

modes, shown in Figure 2b, are monitored via three sensors located using the method described in [7], as shown in Figure 2a. Strains for estimating bending moments are measured at the indicated locations (Fig. 2a) at a distance of 5 cm from the rotation axes of the corresponding lockable joints. In the simulations, the measured strains are calculated using shape functions. Proportional damping is selected: $\zeta_1 = 1$ %, $\zeta_2 = 1.75$ %, $\zeta_3 = 3.31$ %, $\zeta_4 = 6.52$ %, $\zeta_5 = 6.94$ %, $\zeta_6 = 9.31$ %, $\zeta_7 = 10$ %, $\zeta_8 = 14.74$ %, $\zeta_9 = 15.87$ %, $\zeta_{10} = 24.50$ %, and $\zeta_{11} = 27.21$ %, where the last vibration mode has an undamped natural frequency of 264 Hz.

The structure is set in motion by an impact, whose location is shown in Figure 2a. The impact is simulated by applying an initial velocity condition of 0.5 m/s to the appropriate degree of freedom. Such an impact excites mainly the second vibration mode.

First, the performance of the proposed methodology in attenuation of vibrations is demonstrated. The weights are selected as $\alpha_p = \omega_p^{-2}$, $t_{\text{lock}} = 2$ ms, $t_{\text{unlock}} = 15$ ms, $\kappa_1 = 0.05$ W, and $\kappa_1 = 2{\cdot}10^{-5}$ W. The results are illustrated in Figure 3. Control signals exhibit the same time histories due to the equal opening angles of the connected beams for each monitored mode shape (Fig. 2b). It is evident that locking the joint leads to efficient energy transfer between vibration modes. Initially, the mechanical energy is primarily transferred from the second, predominantly excited, vibration mode into the higher-order modes. This results in increasing strains. When the mechanical energy accumulates in the higher-order vibration modes, the joints are unlocked, and the energy is released as high-frequency vibration, which is subsequently rapidly dissipated. This is also observable in the time history of strains. In contrast to the PAR approach, the proposed modal approach does not unlock the joint at the first maximal strain value but instead waits for a more opportune moment. This is visible in the time history of strains near $t = 0.2$ s and in the time interval from $0.3$ to $0.4$ s. This operation is repeated several times, resulting in efficient vibration reduction, as evidenced by the displacements at the sensor locations.

In the case of an application dedicated to energy harvesting, the energy is transferred into the first, preselected, vibration mode. This is achieved by setting $\alpha_1 = -5\omega_p^{-2}$, while the other weights and parameters remain the same as in the vibration attenuation case. The results are

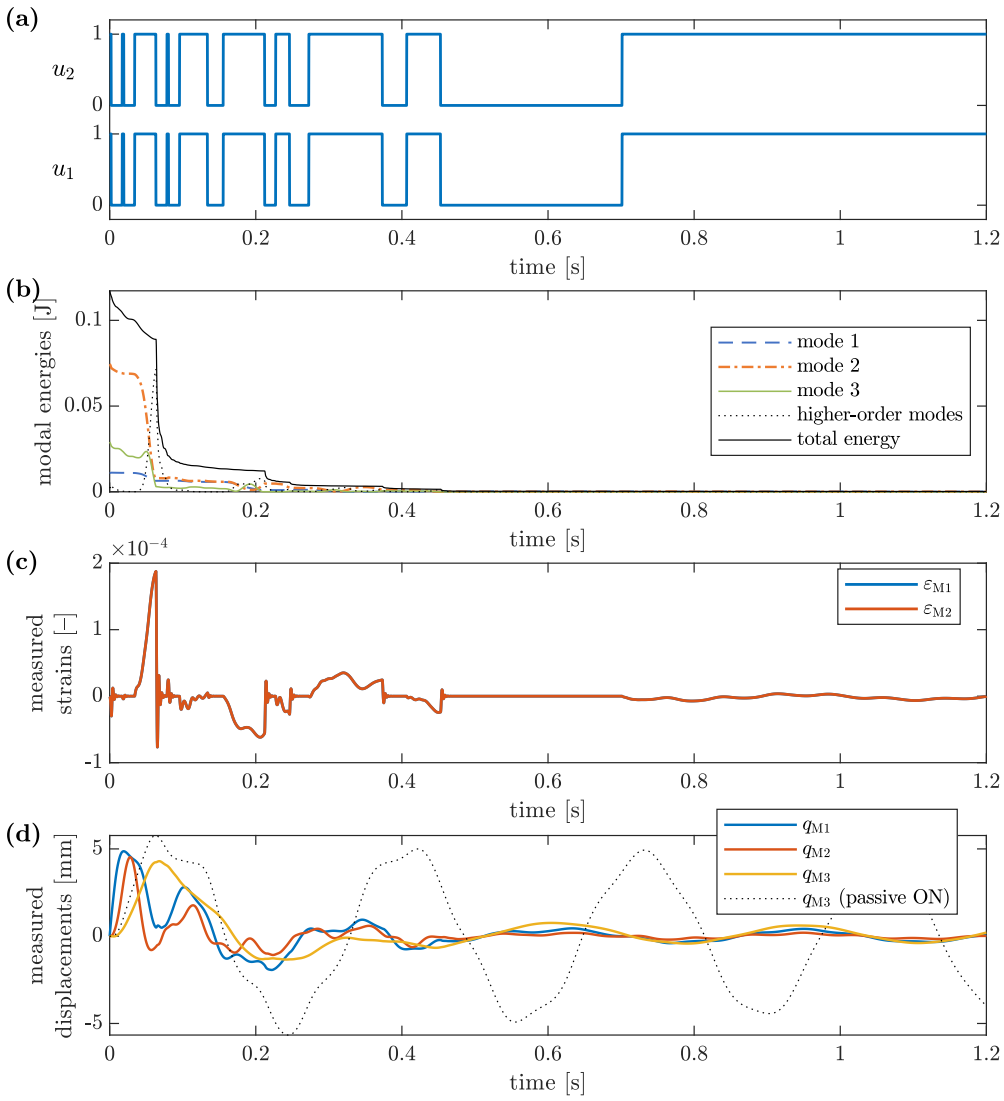


**Figure 3:** Vibration attenuation; time histories of: (a) control signals, (b) total and modal energies, (c) measured strains and (d) structural displacements at sensor locations compared with structure tip displacement in passive ON case (joints locked)

shown in Figure 4. When joints are locked ($u_k(t) = 1$), the energy exchange between modes is visible, but in this case, the algorithm does not unlock the joints at the maximum value of the measured strains. Instead, it unlocks them when the strains are close to zero. This ensures that the energy is not released as free vibration in the higher-order modes (and wasted in this case), but rather transferred into the targeted vibration mode. It is evident that the energy of the targeted (first) vibration mode becomes predominant. Due to the fact that energy is transferred to the first mode, the vibration amplitude becomes larger than in the passive case. Additionally, once again, the control is not sensitive to the local maxima of the strain (Fig. 3a and c).

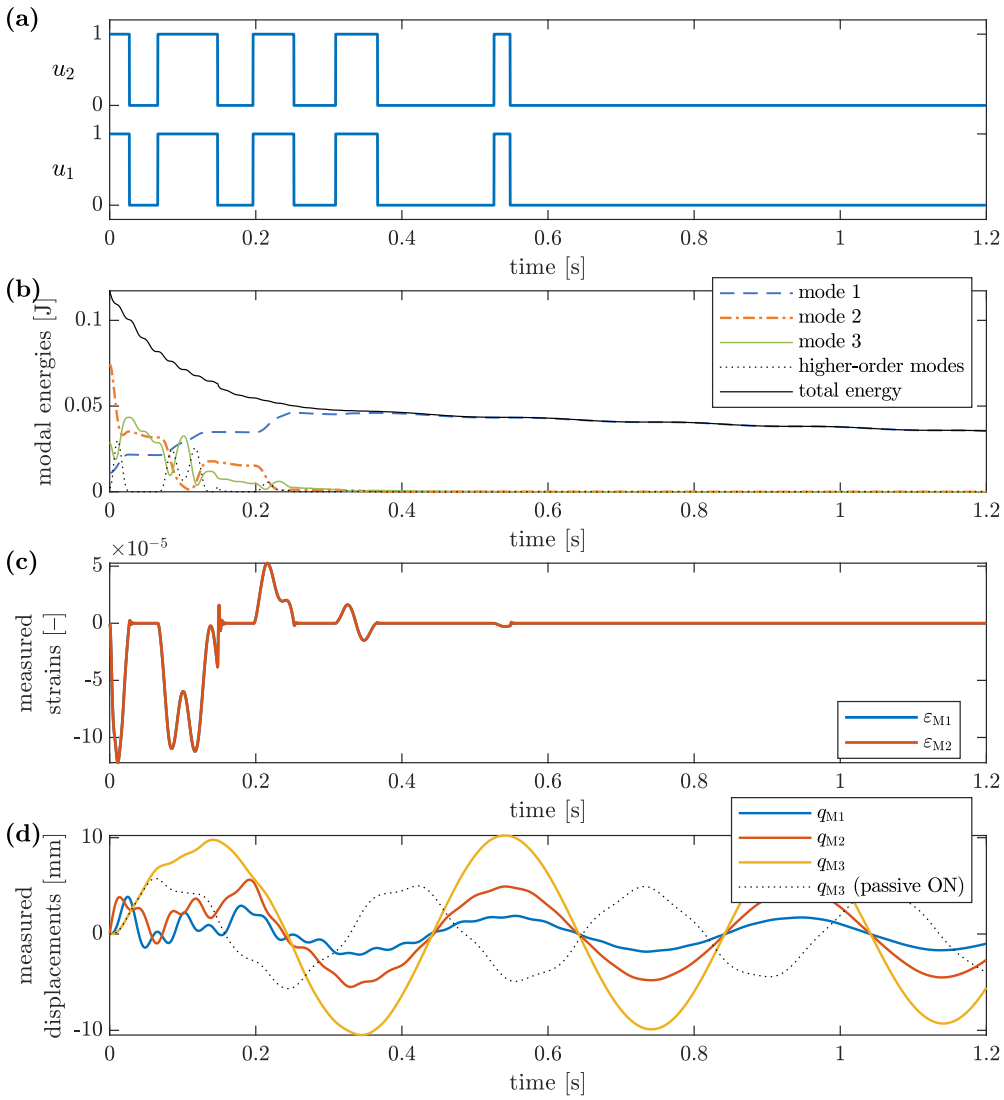


**Figure 4:** Energy transfer to the first vibration mode; time histories of: (a) control signals, (b) total and modal energies, (c) measured strains and (d) structural displacements at sensor locations compared with structure tip displacement in passive ON case (joints locked)

## 5 CONCLUSIONS

The conclusions can be summarized as follows:

– The proposed semi-active control methodology can effectively and precisely transfer mechanical energy between vibration modes.

– The proposed control methodology can be applied for both vibration attenuation (by shifting energy into the well-damped higher-order vibration modes) and energy harvesting (by transferring energy into a mode that cooperates well with the energy harvester).

– Compared to the PAR methodology, the proposed modal approach requires additional sensors, with their number being equal to the number of modal velocities to be estimated. However, the additional insight into the global state of the system reduces the control sensitivity to local maxima of the energy transferred to the higher-order vibration modes.

## 6 ACKNOWLEDGEMENTS

This research was funded in whole or in part by the National Science Centre, Poland, under the grant agreement 2020/39/B/ST8/02615. For the purpose of Open Access, the authors have applied a CC-BY public copyright licence to any Author Accepted Manuscript (AAM) version arising from this submission.

## REFERENCES

[1] F. Casciati, G. Magonette, and F. Marazzi, *Technology of Semiactive Devices and Applications in Vibration Mitigation*. John Wiley & Sons, Ltd, 2006. [Online]. Available: https://doi.org/10.1002/0470022914

[2] L. Gaul, H. Albrecht, and J. Wirnitzer, "Semi-Active Friction Damping of Large Space Truss Structures," *Shock and Vibration*, vol. 11, pp. 173–186, 2004. [Online]. Available: https://doi.org/10.1155/2004/565947

[3] S. Laflamme, D. Taylor, M. Abdellaoui Maane, and J. J. Connor, "Modified friction device for control of large-scale systems," *Structural Control and Health Monitoring*, vol. 19, no. 4, pp. 548–564, 2012. [Online]. Available: https://doi.org/10.1002/stc.454

[4] A. Mróz, J. Holnicki-Szulc, and J. Biczyk, "Prestress Accumulation-Release Technique for Damping of Impact-Born Vibrations: Application to Self-Deployable Structures," *Mathematical Problems in Engineering*, vol. 2015, p. 720236, 2015. [Online]. Available: https://doi.org/10.1155/2015/720236

[5] B. Popławski, G. Mikułowski, A. Mróz, and Ł. Jankowski, "Decentralized semi-active damping of free structural vibrations by means of structural nodes with an on/off ability to transmit moments," *Mechanical Systems and Signal Processing*, vol. 100, pp. 926–939, 2018. [Online]. Available: https://doi.org/10.1016/j.ymssp.2017.08.012

[6] M. Ostrowski, B. Błachowski, B. Popławski, D. Pisarski, G. Mikułowski, and Ł. Jankowski, "Semi-active modal control of structures with lockable joints: general methodology and applications," *Structural Control and Health Monitoring*, vol. 28, no. 5, p. e2710, 2021. [Online]. Available: https://doi.org/10.1002/stc.2710

[7] B. Błachowski, A. Świercz, M. Ostrowski, P. Tauzowski, P. Olaszek, and Ł. Jankowski, "Convex relaxation for efficient sensor layout optimization in large-scale structures subjected to moving loads," *Computer-Aided Civil and Infrastructure Engineering*, vol. 35, no. 10, pp. 1085–1100, 2020. [Online]. Available: https://doi.org/10.1111/mice.12553